Band-Edge Properties of Quasi-One-Dimensional HgTe-CdTe Heterostructures

J. R. Meyer, F. J. Bartoli, and C. A. Hoffman
Naval Research Laboratory, Washington, D.C. 20375

L. R. Ram-Mohan
Worcester Polytechnic Institute, Worcester, Massachusetts 01609
(Received 14 November 1989; revised manuscript received 29 January 1990)

We discuss a number of potential advantages offered by materials with very narrow energy gaps in the study of quasi-one-dimensional physics. Besides the expectation of quite large subband splittings, we predict several new phenomena which have no analog in wide-gap structures, such as the opening of a confinement-induced energy gap in semimetallic structures, a strong decrease of the gap with magnetic field, and ballistic conductance per channel in fractional units of $e^2/\pi\hbar$.

PACS numbers: 73.20.Dx, 73.60.Cs

There has quite recently emerged an intense interest in the properties of quasi-one-dimensional semiconductor devices. In this Letter, we consider theoretically the consequences of introducing lateral confinement into a heterostructure with very narrow energy gap, such as HgTe-CdTe. Not only does the small effective mass in the confinement direction lead to extremely large subband splittings, but we also predict the occurrence of several new effects which do not occur in wide-gap quasi-1D systems.

We consider a quasi-2D (quantum well) or anisotropic 3D (superlattice) system whose energy dispersion in the absence of lateral confinement is $\epsilon[k_\rho,k_z]$, where $k_\rho \equiv (k_x^2+k_y^2)^{1/2}$. We next introduce infinite potential barriers at $x=\pm w/2$, where w is large enough that the lateral confinement may be considered a small perturbation. Resonance states may be found by assuming specular reflection each time an electron strikes one of the barriers. As long as the mean free path Λ is much longer than w, the electron wave function will destructively interfere with itself unless k_x times the round-trip distance, $2w$, is an integral multiple of 2π. That is

$$E_n^{1D}(k_y,k_z) \approx \epsilon[k_x'=(n+1)\pi/w,k_y,k_z]\,. \tag{1}$$

For parabolic dispersion, Eq. (1) yields

$$E_n^{1D} \rightarrow \frac{(n+1)^2\pi^2\hbar^2}{2m_y w^2}+\frac{\hbar^2k_y^2}{2m_y}+\frac{\hbar^2k_z^2}{2m_z}\,, \tag{2}$$

whose first term is the familiar result for confinement in an infinite square well.

An alternative method for introducing spatial confinement in the x-y plane of the unperturbed starting material is to simply apply a magnetic field along the z axis. This constrains the electrons to move in cyclotron orbits and the energy levels become

$$E_n^{CR}(k_z,r_0) \approx \epsilon[k_\rho'=(2n+1\pm1)^{1/2}/r_0,k_z]\,, \tag{3}$$

where $r_0=(\hbar/eB)^{1/2}$ is the semiclassical cyclotron orbit radius for the lowest Landau level. We have included spin splitting, using the small-gap relation for the Landé factor: $g\approx m_0/m_y$. [For parabolic bands and ignoring spin, Eq. (3) yields the familiar form $E_n^{CR}=(2n+1)\hbar^2/2m_y r_0^2+\hbar^2k_z^2/2m_z$.] We note that if the spin-split Landau levels for HgTe-CdTe superlattices are estimated using Eq. (3) in conjunction with zero-field dispersion relations $\epsilon[k_\rho,k_z]$ from an eight-band $k\cdot p$ calculation,[1] the results are in excellent qualitative agreement with the more exact results one obtains by formally introducing the magnetic field into the eight-band calculation. This is because the strong coupling between the bands is effectively incorporated through the multiband result for ϵ. The accuracy of Eq. (3) breaks down only when the magnetic field becomes too large to be considered a perturbation. For the same reason, Eq. (1) should yield quite reliable qualitative results for the effects of lateral confinement on narrow-gap heterostructures as long as w is not too small.

Since the application of a magnetic field to a quasi-1D semiconductor leads to the gradual evolution of the subbands into Landau levels,[2,3] it is useful to combine Eqs. (1) and (3) to obtain an approximate expression which includes both lateral confinement and magnetic fields. Besides increasing the level separation and introducing spin splitting, a magnetic field also has the effect of "flattening" out the k_y dispersion. For parabolic bands this has been discussed in terms of a field-dependent effective mass of the form[3] $m_y(B)\rightarrow m_y(B=0)(1+\omega_c^2/\omega_0^2)$, where $\hbar\omega_c$ is the cyclotron resonance energy and $\hbar\omega_0$ is the subband splitting at zero field. Here we alternatively account for the field by substituting $k_y'\rightarrow k_y/[1+(w/\pi r_0)^4]^{1/2}$, which is equivalent to introducing a field-dependent mass in the limit of parabolic bands. We obtain the net result[4]

$$E_n^{1D}(k_y,k_z,r_0) \approx \epsilon\left\{k_x'=\left[\left(\frac{(n+1)^4\pi^4}{w^4}+\frac{(2n+1)^2}{r_0^4}\right)^{1/2}\pm\frac{1}{r_0^2}\right]^{1/2},k_y'=\frac{k_y}{[1+(w/\pi r_0)^4]^{1/2}},k_z\right\}. \tag{4}$$

It is easily verified that Eq. (4) reduces to Eq. (1) in the limit of small magnetic fields ($r_0 \gg w$) and Eq. (3) at high fields ($r_0 \ll w$).

Electron and hole dispersion relations for HgTe-CdTe quantum wells and superlattices have been calculated using an eight-band transfer-matrix ($k \cdot p$) algorithm which has been described in detail elsewhere[1,5] (the valence-band offset is taken to be 350 meV). As a first example of how the multiband ϵ obtained from this calculation can be used in Eq. (4) to estimate band structures for laterally confined narrow-gap heterostructures, we take the starting material to be a HgTe-CdTe single quantum well with thickness $d_W = 78$ Å, which the calculation predicts should have an unperturbed energy gap of 10 meV. If we then impose lateral confinement of width $w = 2000$ Å at zero magnetic field, Eq. (4) yields the subband structure illustrated in Fig. 1. The splittings are much larger than those usually encountered in wide-gap quasi-1D systems ($|E_1 - E_0|$ is 6.0 meV for electrons and 4.4 meV for holes). However, because of nonparabolicity the electron bands are almost evenly spaced rather than increasing as $(n+1)^2$ as predicted by the simplified expression in Eq. (2). Furthermore, the nonparabolicity of the hole band is so strong that the subband spacing actually decreases with n (the extreme nonparabolicity of the hole band in HgTe-CdTe superlattices has been verified experimentally[6]). Since the k_ρ dispersion for holes in the unperturbed quantum well is double valued,[6] the subband energies do not decrease monotonically with n. Similarly, the eight-band calculation verifies that in a magnetic field, the hole Landau-level energies do not monotonically decrease with n. The figure shows that this leads to an extremely large density of states at energies between -30 and -35 meV.

In practical terms, one method for achieving lateral confinement is physical removal (e.g., by etching) of material outside the boundaries of the lateral wall. However, another possibility is to employ a $Hg_{1-x}Cd_xTe$ alloy layer with small energy gap in a metal-insulator-semiconductor (MIS) device with a very narrow gate. Quasi-2D properties of electrons in $Hg_{1-x}Cd_xTe$ have been studied for some time using structures in which a gate-controlled triangular potential well provides the confinement in the z direction.[7] Merkt and co-workers[8,9] have recently successfully applied this approach to the fabrication of laterally confined structures in InSb. Although InSb has a relatively narrow energy gap and hence some of the advantages discussed above, $Hg_{1-x}Cd_xTe$-based structures could be made to have even smaller E_g. Since $Hg_{1-x}Cd_xTe$-based MIS devices with dimensions on the order of 1 μm are at the limits of what is already achievable using conventional optical lithography, it may be possible to fabricate devices displaying quasi-1D properties using only existing technology. Another system of materials whose energy gaps can be tuned very close to zero are the lead and tin chalcogenides, e.g., PbTe-SnTe quantum wells and superlattices.[10] An advantage of this system is that extremely long mean free paths (up to 30 μm in high-quality PbTe[11]) may be possible due to the large static dielectric constant.

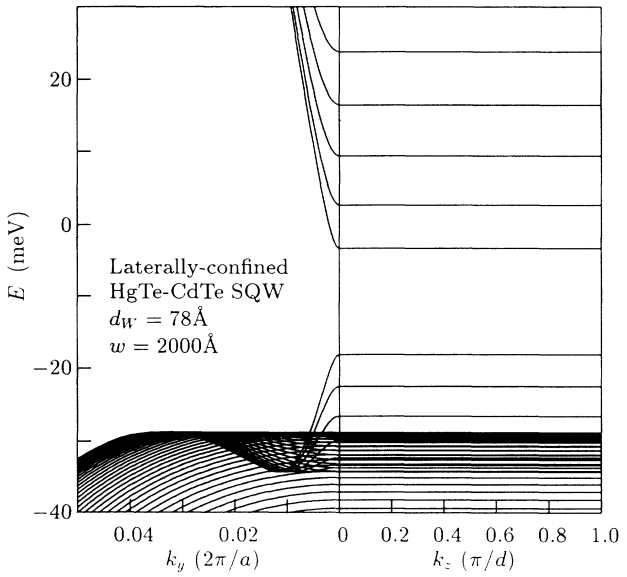

FIG. 1. Dispersion relations along the wire (k_y) and along the growth direction (k_z) for a laterally confined [100] HgTe-CdTe single quantum well at $T = 4.2$ K. The z-direction (d_W) and x-direction (w) well widths are indicated.

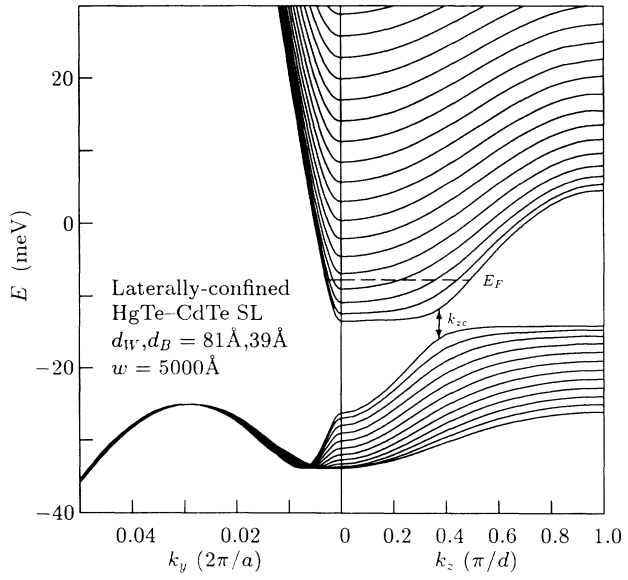

FIG. 2. Dispersion relations along the wire (k_y) and along the superlattice growth direction (k_z) for a laterally confined HgTe-CdTe superlattice at $T = 4.2$ K. The Fermi level E_F for $N_D - N_A = 3 \times 10^{15}$ cm^{-3} and the wave vector k_{zc} at which the E1 and HH1 bands cross in the absence of lateral confinement are indicated. Higher-order hole subbands have been omitted for clarity.

Having discussed some potential advantages of using very-narrow-gap quasi-1D structures to study processes which have already been identified and investigated in wide-gap devices, the remainder of this Letter will be concerned with phenomena which are unique to narrow-gap and zero-gap laterally confined systems. We consider in Fig. 2 the case where a semimetallic HgTe-CdTe superlattice is employed as the starting material rather than a single quantum well. Note that in contrast to Fig. 1, there is now dispersion in k_z since the superlattice barriers are thin enough to allow significant interwell interactions. In fact, the lowest electronlike (E1) and the highest holelike (HH1) subbands anticross at an intermediate wave vector, $k_{zc} \approx 0.4\pi/d$ (d is the superlattice period). As has been discussed previously for HgTe-CdTe superlattices without lateral confinement,[5,6] one finds that the conduction-band minimum extends roughly between $k_z = 0$ and k_{zc} while the valence-band maximum spans the region k_{zc} to π/d. However, whereas HgTe-CdTe superlattices with a broad range of d_W are essentially semimetallic,[6] lateral confinement induces an energy gap in quasi-1D structures. Although E_g is only 0.6 meV in the present example since w is relatively large (5000 Å), much larger gaps can result at smaller w (see Fig. 3 below). For both carrier types, the effective mass in the k_y direction depends on $E_g(k_z)$, which is seen to vary considerably across the zone.[6] One consequence of this "mass broadening" is that the subband splittings are a relatively strong function of k_z.

The band structure in Fig. 3 employs the same superlattice as in Fig. 2 for the unconfined starting material, but with w decreased to 1000 Å. The solid curves (zero magnetic field) indicate that both the subband splittings (13 meV for electrons) and the confinement-induced energy gap (11 meV) considerably exceed those in Fig. 2. These separations are so large that one expects strong qualitative effects on the experimental properties (e.g., see Fig. 4 below). The dashed curves represent spin-split k_z dispersion relations at $B = 1$ T. We find that the application of a magnetic field leads to a significant reduction of E_g (to 4 meV in this example). Such a reduction must occur, since in the high-field limit the band structure must revert to its form in the absence of confinement. [Equation (4) predicts that E_g should vanish in the large-B limit.[12]] The spin splittings are also quite large (15 meV for the ground-state electrons) due to the inverse dependence on effective mass. This is also why Alsmeier, Sikorski, and Merkt[8] have succeeded experimentally in identifying spin splitting for quasi-1D InSb, while spin effects have been much more difficult to observe in laterally confined GaAs-based structures.

Magnetotransport studies on semimetallic HgTe-CdTe superlattices have demonstrated that thermally generated intrinsic electrons and holes are readily observable down to temperatures as low as 15 K.[6] Clearly, the energy gap induced by lateral confinement in quasi-1D structures and its variation with magnetic field should strongly affect the concentrations of these carriers. A statistical calculation using the band structure shown in Fig. 3 and assuming twenty superlattice periods yields the temperature-dependent carrier densities illustrated in Fig. 4. Here n and p are given in both 1D units (density

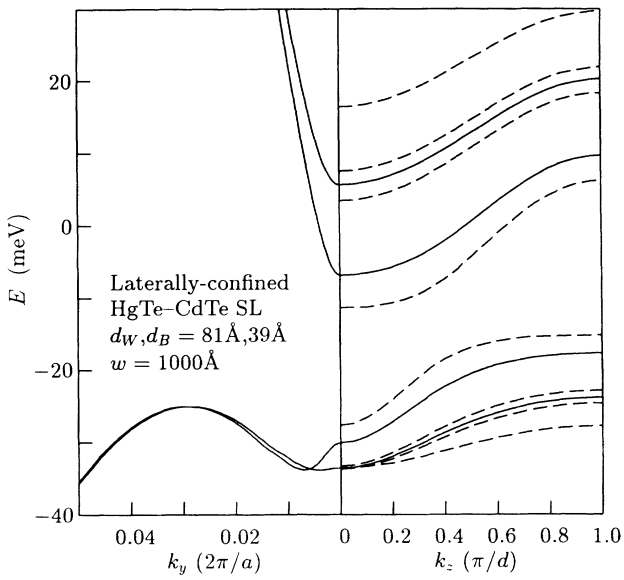

FIG. 3. Dispersion relations along the wire and along the growth direction for a laterally confined HgTe-CdTe superlattice at $T = 4.2$ K (only the $n = 0$ and $n = 1$ subbands are shown). Dashed curves represent k_z dispersion for the spin-split subbands at a magnetic field of 1 T (for both electrons and holes, the order is 0^-, 0^+, 1^-, 1^+).

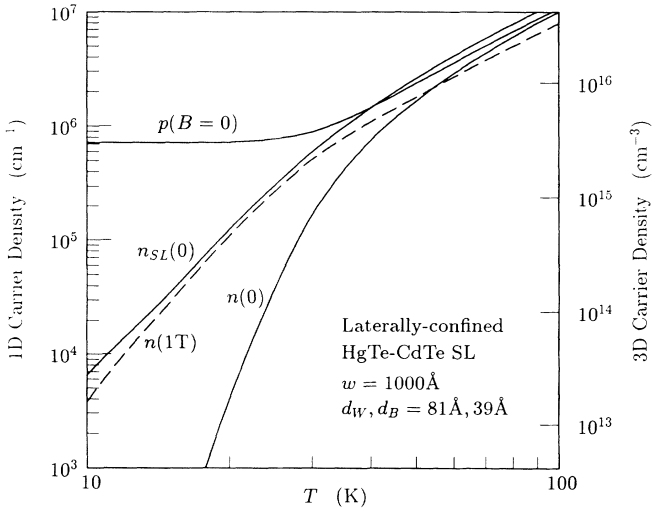

FIG. 4. Electron and hole densities vs temperature, for a laterally confined HgTe-CdTe superlattice. The 3D net acceptor concentration is taken to be $N_A - N_D = 3 \times 10^{15}$ cm^{-3}, and the 1D densities are based on a twenty-period superlattice ($t \approx 2400$ Å) with lateral-confinement width $w = 1000$ Å. Minority electron densities with and without a magnetic field are given, and n_{SL} is the electron density for the same superlattice in the absence of lateral confinement.

per unit wire length) and equivalent 3D units ($n^{3D} \equiv n^{1D}/wt$, where $t \approx 2400$ Å is the total thickness in the z direction). Assuming a p-type sample, the Fermi level has been determined by requiring that the net hole density $p^{1D} - n^{1D}$ be fixed at 7.2×10^5 cm^{-1}, which corresponds to a 3D net acceptor concentration of 3×10^{15} cm^{-3} [typical unintentional doping levels in present HgTe-CdTe superlattices[6] tend to fall in the range (3×10^{14})-(1×10^{16}) cm^{-3}]. Figure 4 shows that due to the confinement-induced gap, the intrinsic electron density at low temperatures and zero magnetic field [$n(0)$] is orders of magnitude lower than that for an unpatterned superlattice with the same specifications [$n_{SL}(0)$]. Note that the suppression of n in the laterally confined structure continues well into the temperature region where the intrinsic concentration is comparable to the background doping level. On the other hand, the application of a magnetic field leads to a strong increase in the low-temperature minority electron concentration, due to the decrease of E_g with increasing B. The figure shows that at $T = 15$ K, the electron density at $B = 1$ T exceeds the zero-field value by well over 2 orders of magnitude. While one also expects n_{SL} to increase with magnetic field, the predicted dependence is not nearly as strong. Such dramatic variations with w and B should provide easily identifiable signatures of the lateral confinement. Furthermore, the large subband splittings in the present system should yield manifestations of the quasi-1D band structure at temperatures much higher than those for which 1D effects have been reported in wider-gap lateral-confinement devices.

We finally note that the unusual band structure of quasi-1D semimetallic superlattices will lead to an interesting variation on the quantized ballistic conductance which has been observed in laterally confined GaAs-based structures.[13,14] It is easily shown that in the absence of scattering the conductance becomes

$$G = \frac{N_z e^2}{\pi\hbar} \sum_n f_n(E_F) , \tag{5}$$

where $N_z = t/d$ is the total number of wells in the superlattice, the sum is over subbands, and $f_n(E_F)$ is the fraction of the Brillouin zone for which the bottom of a given band lies below the Fermi level. For a single quantum well Eq. (5) yields the previously derived result[13,14] in which the conductance is quantized in units of $e^2/\pi\hbar$, since $N_z = 1$ and with no k_z dispersion the sum gives an integer equal to the number of occupied subbands. However, in laterally confined semimetallic superlattices such as those illustrated in Figs. 2 and 3, only a portion of a given band may lie below the Fermi level. Consider Fig. 2, in which the dashed line indicates the location of E_F when the net 3D donor concentration is 3×10^{15} cm^{-3}. We see that parts of four electron subbands lie below E_F, and that typically the occupied fraction of each band is $f_n \approx k_{zc}/(\pi/d)$ (this approximation is best when w is relatively wide and the energy separation of the bands is small). Equation (5) becomes

$$\frac{G}{N_z} = \left(\frac{k_{zc}}{\pi/d} \right) n' \frac{e^2}{\pi\hbar} , \tag{6}$$

where n' is the number of partially occupied subbands. Thus the conductance per well is not $n'e^2/\pi\hbar$ but some fraction of that quantity, whose value depends only on how far into the zone the electron and hole bands anticross (mass broadening has little effect). For a p-type structure, the result is the same except that k_{zc} is replaced by $\pi/d - k_{zc}$.

We have shown that the lateral confinement of semiconductor heterostructures with very narrow energy gaps leads not only to quite large subband splittings, but also several new phenomena which have no analog in wide-gap systems. These include the opening of a confinement-induced energy gap in semimetallic structures, a strong decrease of the gap with magnetic field, and ballistic conductance per channel in fractional units of $e^2/\pi\hbar$.

[1]L. R. Ram-Mohan, K. H. Yoo, and R. L. Aggarwal, Phys. Rev. B **38**, 6151 (1988).

[2]S. B. Kaplan and A. C. Warren, Phys. Rev. B **34**, 1346 (1986).

[3]K.-F. Berggren and D. J. Newson, Semicond. Sci. Technol. **1**, 327 (1986).

[4]Since the assumption of a uniformly flattened k_y dispersion becomes inappropriate at large B, Eq. (4) yields the wrong density of states in the high-field limit. We suggest that whenever $r_0 < w/2$, one should take a fraction $1 - 2r_0/w$ of the states to be dispersionless and have the usual Landau density (approximately this fraction will execute cyclotron orbits which do not impact either lateral wall).

[5]J. R. Meyer, R. J. Wagner, F. J. Bartoli, C. A. Hoffman, and L. R. Ram-Mohan, Phys. Rev. B **40**, 1388 (1989).

[6]C. A. Hoffman, J. R. Meyer, F. J. Bartoli, J. W. Han, J. W. Cook, Jr., J. F. Schetzina, and J. N. Schulman, Phys. Rev. B **39**, 5208 (1989).

[7]W.-Q. Zhao, F. Koch, J. Ziegler, and H. Maier, Phys. Rev. B **31**, 2416 (1985).

[8]J. Alsmeier, Ch. Sikorski, and U. Merkt, Phys. Rev. B **37**, 4314 (1988).

[9]U. Merkt, Superlattices Microstruct. **6**, 341 (1989).

[10]G. Bauer and H. Clemens, Semicond. Sci. Technol. (to be published).

[11]L. Palmetzofer, K. H. Gresslehner, L. Ratschbacher, and A. Lopez-Otero, in *Physics of Narrow Gap Semiconductors*, edited by E. Gornik, H. Heinrich, and L. Palmetzhofer, Lecture Notes in Physics Vol. 152 (Springer-Verlag, Berlin, 1982), p. 391.

[12]The eight-band calculation without lateral confinement yields that higher-order effects eventually lead to a field-induced gap at sufficiently large B (2 T in the present example).

[13]B. J. van Wees, H. van Houten, C. W. J. Beenakker, J. G. Williamson, L. P. Kouwenhoven, D. van der Marel, and C. T. Foxon, Phys. Rev. Lett. **60**, 848 (1988).

[14]D. A. Wharam, T. J. Thornton, R. Newbury, M. Pepper, H. Ahmed, J. E. F. Frost, D. G. Hasko, D. C. Peacock, D. A. Ritchie, and G. A. C. Jones, J. Phys. C **21**, L209 (1988).